

Energy-band structure of CoSi_2 epitaxially grown on $\text{Si}(111)$

G. Gewinner, C. Pirri, J. C. Peruchetti, and D. Bolmont

Laboratoire de Physique et de Spectroscopie Electronique, Faculté des Sciences et Techniques—Université de Haute-Alsace, 4, rue des Frères Lumière-68093 Mulhouse Cedex, France

J. Derrien

Centre de Recherche sur les Mécanismes de la Croissance Cristalline, CNRS—Campus de Luminy—Case 913, 13288 Marseille Cedex 9, France

P. Thiry

Laboratoire pour l'Utilisation du Rayonnement Electromagnétique, Université Paris-Sud—91405 Orsay, France

(Received 23 November 1987)

Angle-resolved photoemission experiments performed with synchrotron radiation allow us to map the energy-band structure along the Γ - L symmetry direction of the bulk Brillouin zone for CoSi_2 epitaxially grown on $\text{Si}(111)$. Two kinds of epitaxial crystals with either Co-rich or Si-rich surfaces were investigated in order to identify unambiguously the photoemission transitions from bulk electronic states. Within a direct transition model assuming a free-electron-like final-state band, the experimental band dispersions are in fairly good agreement with a recent self-consistent band-structure calculation for the free-electron-like Λ_1 bands. However, measured binding energies for Co $3d$ -like states such as Γ'_{25} (3.5 eV) and the upper nonbonding Λ_3 band (~ 1.4 eV) are systematically smaller than those calculated (typically by 20% at Γ_{12}). It is suggested that these discrepancies may be explained in terms of correlation effects for band states with strong d character. A distortion of the lower Λ_3 band near L , observed on a $\text{CoSi}_2(111)$ silicon-rich surface, is attributed to a surface-structure-induced effect.

I. INTRODUCTION

In recent years, transition-metal silicides have been widely used in microelectronics technology as Schottky barriers, gate electrodes, interconnects, and contacts.¹⁻³ Among these materials, epitaxial silicides possess several attractive advantages. For example, PtSi ,⁴ Pd_2Si ,⁵ NiSi_2 ,^{6,7} and CoSi_2 ,⁸⁻¹⁴ have been reported to epitaxially grow on the silicon substrate and present regular atomic arrangement at the silicide-silicon interface, permitting therefore basic understanding of the interface physics (crystallographic and electronic structures). Moreover, on top of these epitaxial silicides, it is possible to epitaxially regrow silicon material, opening the way to novel classes of devices based on semiconductor-metal-semiconductor multilayer structures.¹⁵

To achieve these technological applications, a detailed knowledge of the electronic properties of the materials involved in these devices is needed. CoSi_2 is now the most commonly used material in silicon-metal-silicon transistor technology.¹⁶ Yet only a few preliminary photoemission experiments have been devoted to its electronic structure, dealing mainly with its density of states (DOS).^{13,17} The same statement holds also for theory except for two recently published band-structure calculations.^{18,19} To bridge over this lack, we have undertaken the first experimental energy-band structure of CoSi_2 epitaxially grown on $\text{Si}(111)$ by angle-resolved photoemission spectroscopy (ARPES) performed with synchrotron radiation (SR). The paper is organized as follows: The

next section is devoted to some detailed information on the experimental procedure, the third section to results deduced from ARPES spectra, and a comparison with a recent self-consistent calculation performed on CoSi_2 (Ref. 19) is given in the fourth section.

II. EXPERIMENTAL PROCEDURE

Experiments were performed with the Laboratoire pour l'Utilisation du Rayonnement Electromagnétique (LURE-Orsay) synchrotron radiation facilities. $\text{Si}(111)$ wafers were loaded in an uhv chamber equipped with low-energy electron diffraction (LEED), Auger electron spectroscopy (AES), rare-gas ion etching gun, cobalt evaporator, quartz microbalance, and angle-resolved hemispherical electron analyzer.

The uhv chamber was placed on a SR beam line downstream from a wiggler in order to take advantage of its high-flux beam. The photon energies used in these experiments ranged from ~ 10 eV up to ~ 60 eV, and an increment of ~ 1 eV of the photon energy was used for each spectrum. The angular and energy resolution was about 2° and 0.2 eV, respectively, at ~ 20 eV photon energy. With the high-flux beam, ARPES spectra could be recorded very quickly (within a few minutes per spectrum). In this case, contamination by residual pressure (basically in the 10^{-10} torr range) if any, could be minimized. ARPES spectra were recorded in normal emission along the $\langle 111 \rangle$ CoSi_2 axis with a 45° incident beam angle in order to map the bulk energy dispersion curve

$E_i(k)$ along the $\Gamma\Lambda L$ direction of the bulk CoSi_2 Brillouin zone (BZ). Various experimental facilities (off-normal emission, polarization effect of the incident photon with glancing or normal incident angle, etc.) were also used to probe other BZ symmetry points and to determine the symmetry of the investigated bands. The Si(111) surfaces were ion-sputtered and annealed in the conventional manner in order to get clean and ordered Si(111)-(7 \times 7) superstructures as checked with LEED, AES, and ARPES. Co atoms were then evaporated onto the Si substrates maintained at room temperature (RT) and subsequently annealed to temperatures in the 420–500 °C range to epitaxially grow CoSi_2 thin films on Si,^{8,9,13,14} following the so-called template method.²⁰

It is well known that this technique provides us with a CoSi_2 film mainly composed of *B*-type grains although one cannot avoid the formation of some grains of *A* type (in orientation *A*, the CoSi_2 and Si unit cells are aligned in the same sense, whereas in orientation *B* the CoSi_2 is rotated by an angle of 180° about [111] with respect to that in orientation *A*). The fraction of phase *A* on similar samples estimated by electron microscopy does not exceed 20%. Moreover, the solid-phase epitaxy (SPE) technique used here may also induce some pinholes in the CoSi_2 film, as clearly demonstrated recently,²¹ although these holes have no noticeable consequence on the CoSi_2 ARPES spectra.

The primary objective of this work reported here was to investigate the *bulk* electronic properties of CoSi_2 . Previous studies²² have shown that CoSi_2 can be terminated, during its formation, either by Co or by Si topmost atomic planes depending on the annealing temperature. Therefore these Co (or Si) enriched-surface CoSi_2 samples should display different *surface* states but identical *bulk* states with ARPES technique. Using this ap-

proach we have prepared two kinds of CoSi_2 samples of total thickness ~ 30 Å. The first ones (obtained by SPE at ~ 420 °C), hereafter called $\text{CoSi}_2(111)\text{-Co}$ samples, are probably terminated by a Co atomic plane at its topmost surface, and the second ones (obtained by SPE at ~ 540 °C), hereafter called $\text{CoSi}_2(111)\text{-Si}$ samples, by a Si topmost double layer. The ARPES spectra from both surfaces will be discussed below.

III. RESULTS

Figure 1 shows the standard ARPES experimental geometry, including the Brillouin zone of a fcc crystal (CoSi_2 structure).

Figures 2 and 3 display some typical ARPES spectra of a $\text{CoSi}_2(111)\text{-Co}$ and a $\text{CoSi}_2(111)\text{-Si}$ sample, respectively. These ARPES spectra were recorded at normal emission (polar angle $\theta=0^\circ$) in the $\Gamma L K U$ plane with a fixed light incident angle ($\alpha=45^\circ$) and various photon energies.

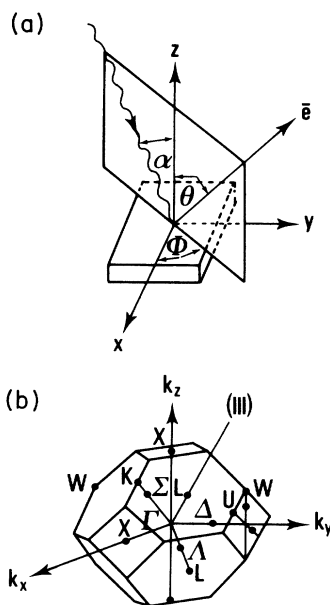


FIG. 1. (a) shows the standard ARPES experimental geometry. (b) shows the Brillouin zone of a fcc crystal.

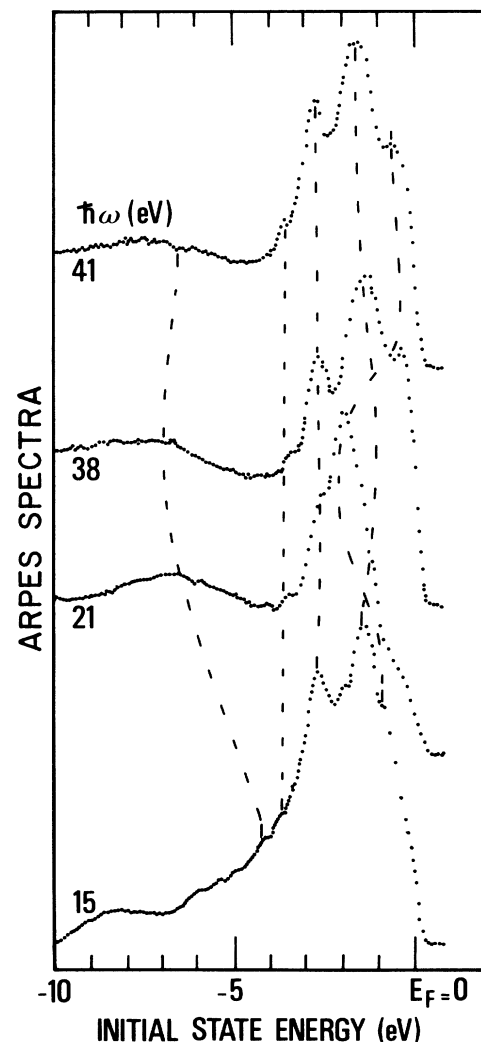


FIG. 2. Some typical ARPES spectra recorded at normal emission on a $\text{CoSi}_2(111)$ sample, the topmost surface of which is terminated by a Co atomic plane [$\text{CoSi}_2(111)\text{-Co}$ sample].

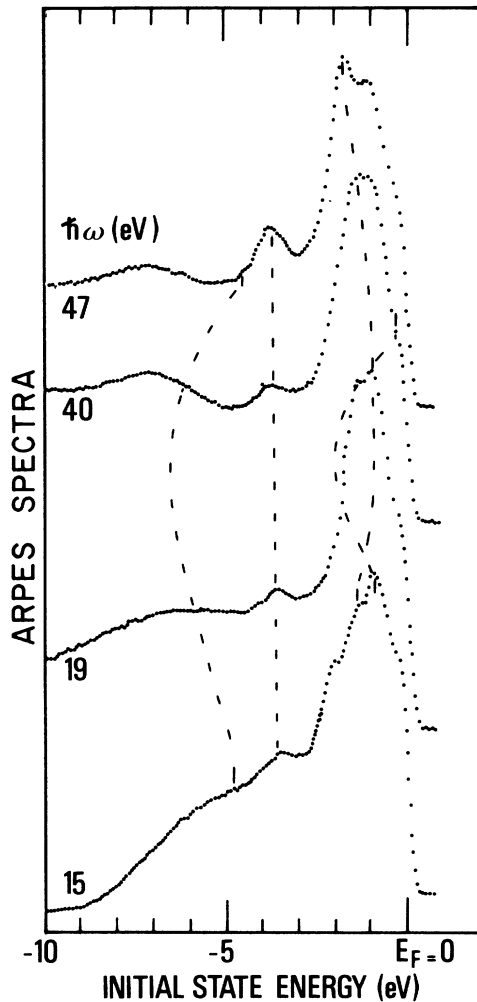


FIG. 3. Same as in Fig. 2. The CoSi₂(111) sample is now terminated by a Si topmost double layer [CoSi₂(111)-Si sample].

According to the commonly accepted photoemission model, the components of crystal momentum \mathbf{k} , parallel to the surface (k_{\parallel}) of the excited electron, are conserved during its ejection into vacuum, and electron energies are also related by the conservation law

$$E_f = E_i + \hbar\omega,$$

$$E = E_f - \phi,$$

where E_f and E_i are the final and initial electron state in the sample, E is the kinetic energy of the electron photoemitted in vacuum, $\hbar\omega$ is the incident photon energy, and ϕ is the sample work function.

In order to map the $E_i(k)$ dispersion of the initial-state bands, we adopt the commonly accepted direct transition model and use the conventional single free-electron final band dispersion. In this case, from conservation laws of energy and momentum, one can readily determine the k_{\perp} component of crystal momentum for a given transition.

Within this model, the only adjustable parameter is the crystal inner potential V_0 locating the free-electron final parabola with respect to the vacuum level. m is taken to be the free-electron rest mass in the following analysis.

For cubic crystals, it has been shown²³ that in ARPES spectra recorded at normal emission, only Λ_1 and Λ_3 symmetry initial states can be probed along Λ . We interpret therefore our data on the basis of these selection rules and direct transition photoemission model. The determination of the Λ_1 and Λ_3 band symmetry has been achieved using the polarization effect of the SR beam (mainly s or p polarization depending on normal or glancing incidence of light).

In Figs. 4 and 5 are plotted experimental energy band dispersion curves along the $\Gamma\Lambda L\Lambda\Gamma$ direction for the CoSi₂-Co and CoSi₂-Si samples, respectively. These dispersions have been mapped choosing the crystal inner potential V_0 to yield the best symmetry of the Λ_1 band dispersion curve, which lies just below the Fermi level, around the L high-symmetry point. This procedure yields $V_0 \approx 14.8$ eV to be compared to the one found on

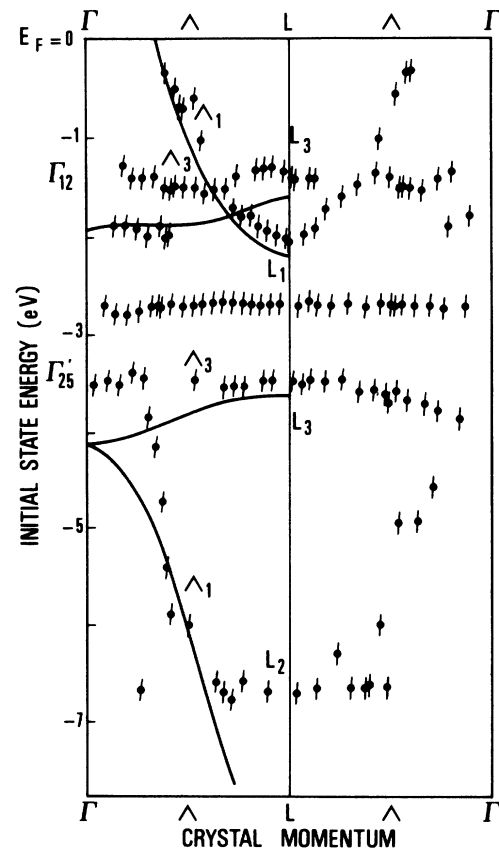


FIG. 4. Electronic band structure of CoSi₂(111)-Co sample along the $\Gamma\Lambda\Gamma$ direction. Dots are deduced from data. Solid lines are from LMTO ASA calculations according to Ref. 19, reported here for a comparison. Four bands, Λ_1, Λ_3 , are observed in the range 0 to -7 eV. They display a quasiperfect symmetry around the L point and agree qualitatively with theory. Note however the large discrepancies, as far as the energy location is concerned, between theory and data for the upper Λ_3 band and at the Γ'_{25} point where d orbital character is large. A surface state band is observed at -2.7 eV. Other weak features at -2 eV are assigned to a one-dimensional density-of-states effect and umklapp processes.

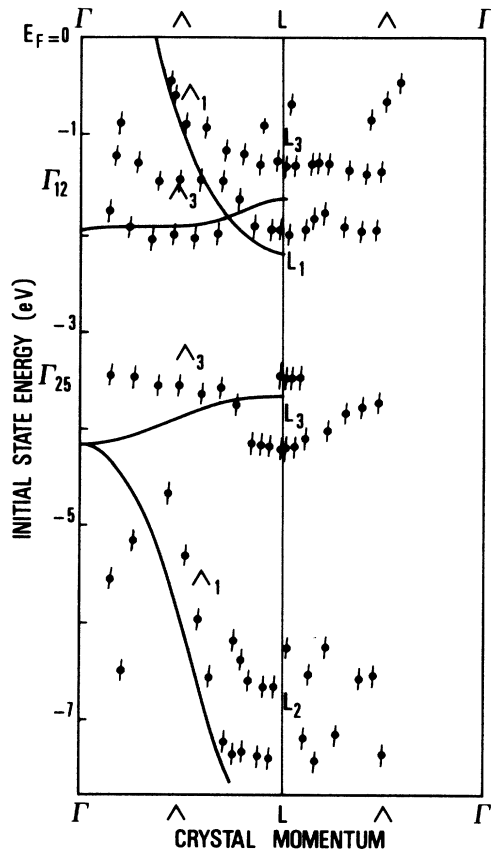


FIG. 5. Electronic band structure of the $\text{CoSi}_2(111)\text{-Si}$ sample along the $\Gamma L \Gamma$ direction. As in Fig. 4, the same conclusions concerning the theory-versus-data comparison remain valid. No surface-state band is observed now at -2.7 eV. In contrast, a strong distortion of the lower Λ_3 band is clearly seen at the L_3 point and assigned to a surface-state-induced effect.

NiSi_2 ($V_0 \sim 14.2$ eV), another disilicide similar to CoSi_2 .²⁴ The energy band dispersion has been plotted using mainly the normal emission ARPES spectra (Figs. 2 and 3), although for several high-symmetry points (Γ and L) we have also included some data recorded at off-normal emission in order to check the reliability of our experiments. All initial-state band energies in Figs. 4 and 5 are referred to the Fermi level (0 eV).

IV. DISCUSSION

Recently Lambrecht *et al.* published a self-consistent band-structure calculation for CoSi_2 using the linear-muffin-tin-orbitals atomic-sphere approximation (LMTO-ASA) to solve the Kohn-Sham density functional equations.¹⁹

The theoretical bands along ΓL have been reproduced (solid line in Figs. 4 and 5) for comparison with our CoSi_2 data (dots). In principle, one expects that a given bulk

transition should be observed in the relevant ARPES spectra of both kinds of $\text{CoSi}_2(111)$ surfaces (Figs. 2 and 3). Thus $E_i(k)$ dispersion curves, common in Figs. 3 and 4, i.e., to both investigated samples ($\text{CoSi}_2\text{-Co}$ and $\text{CoSi}_2\text{-Si}$) should correspond to *bulk* states. Indeed we found four bands (Λ_1 and Λ_3) ranging from the Fermi level (0 eV energy) down to ~ -7 eV. These bands have similar dispersion and the same symmetry predicted by theory [compare dots (data) to solid line (theory) in Figs. 4 and 5]. In agreement with theory, there are two Λ_1 and two Λ_3 bands observed predominantly at grazing and near normal incidence respectively. The upper Λ_1 and Λ_3 bands (0 to ~ -2 eV) are very easily observed (Figs. 2 and 3), and are identical for both samples.

The present interpretation based on direct transitions in ARPES spectra is found to be valid up to $\hbar\omega \sim 40$ eV. With higher photon energy, a DOS regime seems to take place, probably due to the fact that the electron mean free path becomes comparable to the thickness of the Co- (or Si-) enriched surface region of the samples. In these cases, the direct transition photoemission model breaks down. Also the contributions of umklapp processes increase progressively with higher photon energies and complicate considerably the interpretation of the spectral features. One-dimensional density-of-states effects are also observed at low photon energies $\hbar\omega < 20$ eV near -2 eV, as can be seen in Figs. 4 and 5. These transitions, which do not conserve the k_1 component, reflect the maximum of the one-dimensional density of states along ΓL due to the presence of the upper Λ_1 band bottom at -2.05 eV. The origin of a few other weak transitions near -0.9 eV on the $\text{CoSi}_2\text{-Si}$ sample and in the -5 to -7 eV range on both kinds of samples, is not yet clear at present.

We have contrived to fully describe the $\Gamma L \Gamma$ line of the extended Brillouin zone and to check the nearly perfect symmetry of the upper Λ_1 band around the L point. The agreement with theory is remarkable, at least as far as the upper Λ_1 band dispersion behavior is concerned. A shift to lower energy is observed between theory and data for the upper Λ_3 band and will be explained later. Integration of these upper bands over the whole k range should yield a large contribution to the DOS observed in an integrated photoemission spectrum in the 0–2-eV energy range. In particular, the upper flat Λ_3 band (~ -1.5 eV) integration over k yields a major contribution to the so called “nonbonding Co 3d states” peak observed in the CoSi_2 DOS.¹³ Indeed, the upper Λ_3 band mainly comes from d orbitals ($\sim 94\%$ at Γ_{12} of Ni 3d electrons in the comparable compound NiSi_2 according to Ref. 25) and its small dispersion along ΓL confirms the quasi-pure- d -orbital character of this band. The behavior of the upper Λ_1 band is quite different. It displays a quasiparabolic dispersion along ΓL and corresponds rather to a mixture of Si and Co s , p , and d electrons (free-electron-like dispersion). The lower Λ_3 and Λ_1 bands (-3.5 to -7 eV) qualitatively reflect also the same dispersion behavior as predicted by calculation. The lower Λ_3 band (-3.5 eV at Γ'_{25}) still has a strong d character at Γ'_{25} [about 70% d character at Γ'_{25} in NiSi_2 (Ref.

25)], but contains an important admixture of Si 3s3p states along ΓL . This band provides an important contribution to the so-called "bonding states" feature in the CoSi₂ DOS,¹³ while the lower Λ_1 band (−3.5 to −7 eV) is a combination of Si and Co electron states with strong free-electron-like *sp* character except near Γ'_{25} .

The feature at −2.7 eV only observed on CoSi₂ samples with a Co enriched surface shows no dispersion with photon energy and has no counterpart in the calculated bulk bands. In agreement with a previous investigation,²⁶ this peak has to be interpreted as a true *surface* state on CoSi₂(111)-Co. It displays some remarkable properties, such as an oscillatory behavior in intensity with k_{\perp} along ΓL . This will be discussed in detail in a separate report devoted to the surface electronic structure of CoSi₂.²⁷

Let us concentrate here on the bulk bands identified in the above discussion. While qualitatively there is a satisfactory accord with theory, it is clear that from a quantitative point of view very important discrepancies can be observed. For instance, measured critical-point initial-state energies at Γ'_{25} (−3.5 eV), L_3 (−1.3 eV), and L_1 (−2.05 eV) are systematically higher than their calculated counterparts. The difference is typically about 20% for the upper Λ_3 band or near Γ'_{25} . At L_1 or near the lower L_3 critical points, the discrepancy is much lower but still larger than the experimental uncertainties. In contrast, the agreement is quite good for most parts of the upper Λ_1 band. The determination of the lower Λ_1 band dispersion is difficult from an experimental point of view. As usually observed, the hole lifetime in the low-lying Λ_1 band becomes rather short because of the great number of available Auger transitions. Thus the photoemission peaks are very broad and the experimental band dispersion is difficult to observe, particularly for rapidly dispersing *s-p* states with a low photoionization cross section. Keeping in mind the orbital content of the various bands discussed above, it is apparent that the stronger the Co 3*d* contribution to a given band state is, the larger the discrepancy between calculated and measured initial-state energy. For instance, the difference between experiment and theory is the largest for the upper Λ_3 band, which has essentially pure Co 3*d* character since it corresponds to the nonbonding Co 3*d* states. Also near Γ'_{25} , the Co 3*d* character is quite dominant. We believe that these discrepancies are not due to the specific photoemission model (free-electron final band) since a more sophisticated final band would not modify the critical-point energies. Actually, this behavior is not surprising because it is well known that a *d*-band narrowing is currently observed for 3*d*-series transition metals such as Ni,²⁸ Co,²⁹ or Cr.³⁰ In these cases, it is well established that the density-functional theory gives a good description of the ground-state properties but not the excitation energies.

The present study strongly suggests that similar effects, due to *d* orbitals, occur in the 3*d* series transition-metal compounds. Self-energy effects indeed shift the measured initial-state energy towards the Fermi level as compared to the calculated one. The magnitude of the shift increases with the *d*-orbital content as well as the binding energy.³¹ These correlation effects are improperly taken into account in standard self-consistent band-structure

calculations and explain the theory-data discrepancies observed for the upper Λ_3 band and at Γ'_{25} (large *d*-orbital character). They explain also why the agreement is very good for the high lying Λ_1 band (low *d*-orbital character). Since the *d*-orbital content varies with *k*, the correlation effects result in a distortion of the bands with respect to standard calculated band-structure results.

In a previous study concerning Cr metal, the experimentally determined band distortions could be reproduced very well by taking explicitly these correlation effects into account.³⁰ Note also that the importance of intra-atomic correlation effects in the case of Ni and Cr silicides has been emphasized previously.³²

Finally it is interesting to note that the dispersion curves for the lower Λ_3 band obtained on CoSi₂(111)-Co and CoSi₂(111)-Si are not identical around the *L* critical point. Since there is only one definite bulk band, this means that a surface structure induced distortion occurs for either one or even both kinds of surfaces. Actually we believe that the correct bulk band dispersion is measured on CoSi₂(111)-Co because of the following observations. While for CoSi₂(111)-Si normal emission spectra show only one peak corresponding to L_3 at −4.2 eV, off-normal spectra probing the *L* point exhibits two candidate peaks for the lower L_3 critical energy at −3.5 and −4.2 eV. Since the −3.5 eV peak corresponds to the energy also measured on CoSi₂(111)-Co, we conclude that this is the relevant L_3 critical point energy. Thus the −4.2 eV peak is attributed to the surface electronic structure associated with segregated Si.²⁷ At the surface, segregated Si species not bonded to Co atoms as in CoSi₂ bulk represent a strong perturbation in the crystal properties. As a matter of fact, direct transitions from bulk states are usually stronger and more easily identified on CoSi₂(111)-Co than on CoSi₂(111)-Si samples.

V. CONCLUSION

We have contrived to plot the first experimental band structure of CoSi₂ epitaxially grown on Si(111) thanks to synchrotron facilities. Our results can be compared favorably to a recent self-consistent energy-band calculation using the LMTO density-functional approach. All energy dispersion features and orbital characters of bands mapping along the ΓL line of the Brillouin zone are found to agree qualitatively with theory. In particular, *sp* derived bands are much better described by standard band calculation than *d*-like states apparently because of the atomic character of the latter, as already demonstrated by previous studies of 3*d* transition metals.

Here one may question why correlation effects are so important in CoSi₂, which exhibits an electronic structure similar to that of a noble metal such as Cu, where correlation effects are found to be of minor importance.³³ Actually the similarity in electronic structure (density of occupied states) between Cu and CoSi₂ is only apparent since for CoSi₂ the *d* character is still very pronounced in the states near the Fermi level and above, because of the strong Co 3*d* hybridization with Si 3s3p states and the

formation of antibonding states in contrast to Cu metal. Thus while the ground state in Cu is the closed-shell $3d^{10}$ configuration, this should not be the case for Co in CoSi_2 , which has rather an open-shell configuration similar to transition metals at the end of the $3d$ series, where correlation effects are very important.

ACKNOWLEDGMENTS

The experiments have been performed with the synchrotron radiation facilities at LURE-Orsay. Technical help from its staff members (G. Jezequel, J. Bonnet, and R. Pinchaux) is greatly appreciated.

-
- ¹K. N. Tu and J. W. Mayer, in *Thin Films—Interdiffusion and Reactions*, edited by J. M. Poate, K. N. Tu, and J. W. Mayer (Wiley, New York, 1978).
- ²S. P. Murarka, *J. Vac. Sci. Technol.* **17**, 775 (1980).
- ³M. A. Nicolet and S. S. Lau, in *Materials and Process Characterization*, edited by N. G. Einspruch and G. B. Larrabee (Academic, New York, 1983).
- ⁴H. Ishiwara, K. Hikosaka, and S. Furukawa, *J. Appl. Phys.* **50**, 5302 (1979).
- ⁵J. L. Freeouf, G. W. Rubloff, P. S. Ho, and T. S. Kaun, *Phys. Rev. Lett.* **43**, 1836 (1979).
- ⁶H. Ishiwara, in *Proceedings of the Symposium on Thin Film Interfaces and Interaction*, edited by J. E. Baglin and J. M. Poate (Electrochemical Society, New Jersey, 1980).
- ⁷K. C. R. Chiu, J. M. Poate, J. E. Rowe, T. T. Sheng, and A. G. Cullis, *Appl. Phys. Lett.* **38**, 988 (1981).
- ⁸S. Saitoh, H. Ishiwara, and S. Furukawa, *Appl. Phys. Lett.* **37**, 203 (1980).
- ⁹J. C. Bean and J. M. Poate, *Appl. Phys. Lett.* **37**, 643 (1980).
- ¹⁰J. M. Gibson, J. C. Bean, J. M. Poate, and R. T. Tung, *Appl. Phys. Lett.* **41**, 818 (1982).
- ¹¹L. J. Chen, J. W. Mayer, and K. N. Tu, *Thin Solid Films* **93**, 135 (1982).
- ¹²J. M. Gibson, J. C. Bean, J. M. Poate, and R. T. Tung, *Thin Solid Films* **93**, 99 (1982).
- ¹³C. Pirri, J. C. Peruchetti, G. Gewinner, and J. Derrien, *Phys. Rev. B* **29**, 3391 (1984).
- ¹⁴J. Derrien, *Surf. Sci.* **168**, 171 (1986), and references therein.
- ¹⁵See, for instance, K. L. Wang, *Solid State Technol.* **26**, 137 (1985).
- ¹⁶J. Derrien and F. Arnaud d'Avitaya, *J. Vac. Sci. Technol. A* **5**, 2111 (1987).
- ¹⁷A. Franciosi, J. H. Weaver, D. G. Neill, F. A. Schmidt, O. Bisi, and C. Calandra, *Phys. Rev. B* **28**, 7000 (1983).
- ¹⁸R. S. Gupta and S. Chatterjee, *J. Phys. F* **16**, 733 (1986).
- ¹⁹W. R. L. Lambrecht, N. E. Christensen, and P. Blöchl, *Phys. Rev. B* **36**, 2493 (1987).
- ²⁰R. T. Tung, J. M. Gibson, and J. M. Poate, *Appl. Phys. Lett.* **42**, 888 (1983).
- ²¹J. Henz, H. von Känel, M. Ospelt, and P. Wachter, *Surf. Sci.* **189-190**, 1055 (1987).
- ²²C. Pirri, J. C. Peruchetti, D. Bolmont, and G. Gewinner, *Phys. Rev. B* **33**, 4108 (1986); see also S. A. Chambers, S. B. Anderson, H. W. Chen, and J. H. Weaver, *ibid.* **34**, 913 (1986).
- ²³W. Eberhardt and F. J. Himpsel, *Phys. Rev. B* **21**, 5572 (1980).
- ²⁴Y. J. Chang and J. L. Erskine, *Phys. Rev. B* **26**, 7031 (1982).
- ²⁵Y. J. Chabal, D. R. Hamam, J. E. Rowe, and M. Schlüter, *Phys. Rev. B* **25**, 7598 (1982); see also D. M. Bylander, L. Kleinman, K. Mednick, and W. R. Grise, *ibid.* **26**, 6379 (1982).
- ²⁶C. Pirri, J. C. Peruchetti, G. Gewinner, and J. Derrien, *Phys. Rev. B* **30**, 6227 (1984).
- ²⁷C. Pirri, G. Gewinner, J. C. Peruchetti, D. Bolmont, and J. Derrien (unpublished).
- ²⁸F. J. Himpsel, J. A. Knapp, and D. E. Eastman, *Phys. Rev. B* **19**, 2919 (1979); see also G. Treglia, F. Ducastelle, and D. Spanjaard, *ibid.* **12**, 6472 (1980).
- ²⁹D. E. Eastman, F. J. Himpsel, and J. A. Knapp, *Phys. Rev. Lett.* **44**, 95 (1980).
- ³⁰G. Gewinner, J. C. Peruchetti, A. Jaeglé, and R. Pinchaux, *Phys. Rev. B* **27**, 3358 (1983); see also D. Aitel Habti, G. Gewinner, J. C. Peruchetti, R. Riedinger, D. Spanjaard, and G. Treglia, *J. Phys. F* **14**, 1317 (1984).
- ³¹O. Bisi, C. Calandra, U. del Pennino, P. Sassaroli, and S. Valeri, *Phys. Rev. B* **30**, 5696 (1984).
- ³²C. Calandra, O. Bisi, U. del Pennino, S. Valeri, and Y. Xi, *Surf. Sci.* **168**, 164 (1986).
- ³³P. Thiry, D. Chandesris, J. Lecante, C. Guillot, R. Pinchaux, and Y. Petroff, *Phys. Rev. Lett.* **43**, 82 (1979).